CONFIDENTIAL

Copy 324
RM L58A23

NACA RM L58A23

NACA

RESEARCH MEMORANDUM

AERODYNAMIC CHARACTERISTICS OVER A MACH NUMBER RANGE OF 1.40 TO 2.78 OF A ROCKET-PROPELLED AIRPLANE CONFIGURATION HAVING A LOW 52.5° DELTA WING AND AN UNSWEPT HORIZONTAL TAIL

By Alan B. Kehlet

Langley Aeronautical Laboratory
Langley Field, Va.

Classification Changed to Unclassified
Authority: NASA Technical Publications Announcements No. 33
Effective Date: October 28, 1960
MHL

CLASSIFIED DOCUMENT

This material contains information affecting the National Defense of the United States within the meaning of the espionage laws, Title 18, U.S.C., Secs. 793 and 794, the transmission or revelation of which in any manner to an unauthorized person is prohibited by law.

NATIONAL ADVISORY COMMITTEE
FOR AERONAUTICS

WASHINGTON

March 6, 1958

CONFIDENTIAL

NATIONAL ADVISORY COMMITTEE FOR AERONAUTICS

RESEARCH MEMORANDUM

AERODYNAMIC CHARACTERISTICS OVER A MACH NUMBER RANGE OF 1.40 TO 2.78 OF A ROCKET-PROPELLED AIRPLANE CONFIGURATION HAVING A LOW 52.5° DELTA WING AND AN UNSWEPT HORIZONTAL TAIL

By Alan B. Kehlet

SUMMARY

A free-flight investigation of an airplane configuration having a low 52.5° delta wing and an unswept horizontal tail has been conducted over a Mach number range of 1.40 to 2.78. At a fixed tail setting of -3.0°, the trim lift coefficient and angle of attack varied from about 0.12 to 0.04 and 3.8° to 2.0°, respectively. The base drag was approximately 5 percent of the total drag at trim lift.

Lift-curve slope, static longitudinal stability, and damping in pitch were obtained only at Mach numbers of 2.59 to 2.74. Theoretical calculations of lift-curve slope and aerodynamic-center location were in good agreement with experimental results.

INTRODUCTION

A general research program was initiated by the Langley Pilotless Aircraft Research Division to study the aerodynamic characteristics of Mach number 3 rocket-propelled airplane configuration models having various wing plan forms. This program was also to extend the aerodynamic data on previously tested similar configurations from Mach numbers near 2 to Mach numbers near 3. At the time this program was started, however, the highest performing rocket motor available was the 6.25-inch-diameter ABL Deacon rocket motor. The single-stage use of this motor limited the obtainable Mach number to about 2 for nonsustained models and, therefore, staging was required to increase the Mach number to about 3.

The purpose of the test reported in this paper was to determine trim, lift, drag, and longitudinal stability characteristics of an airplane configuration having a low 52.5° delta wing and an unswept horizontal tail. The fuselage consisted of an ogive nose section, cylindrical center section, and a convergent tail section. Mounted on the fuselage, in addition to the wing and horizontal tail, was a canopy and a sweptback vertical tail. Because the pitch disturbing mechanism failed to operate, experimental lift and stability data were obtained only near the maximum Mach number. Data at trim conditions were obtained over the 1.40 to 2.78 Mach number range covered.

The model was flown at the Langley Pilotless Aircraft Research Station at Wallops Island, Va.

SYMBOLS

The system of body axes and the positive values of forces, moments, and angles are shown in figure 1.

a.c.	aerodynamic center
A_L	longitudinal-accelerometer reading, g units
A_N	normal-accelerometer reading, g units
A_T	transverse-accelerometer reading, g units
C_C	chord-force coefficient, $-A_L \frac{W/S}{q}$
C_N	normal-force coefficient, $A_{N,cg} \frac{W/S}{q}$
C_D	drag coefficient, $C_C \cos \alpha + C_N \sin \alpha$
C_l	rolling-moment coefficient, $\frac{M_X}{qSb}$
C_L	lift coefficient, $C_N \cos \alpha - C_C \sin \alpha$

C_m total pitching-moment coefficient about center of gravity, $\frac{M_Y}{qS\bar{c}}$

$C_{p,b}$ base pressure coefficient, $\left(p_b - p_\infty\right)/q$

C_Y side-force coefficient, $A_{T,cg}\frac{W/S}{q}$

$\bar{c}$ mean aerodynamic chord (M.A.C.), ft

g acceleration due to gravity, ft/sec^2

I_X moment of inertia in roll, slug-ft^2

I_Y moment of inertia in pitch, slug-ft^2

I_Z moment of inertia in yaw, slug-ft^2

m mass of model, slugs

M Mach number

M_X rolling moment, $I_X\ddot{\phi}$, ft-lb

M_Y pitching moment, $I_Y\ddot{\theta}$, ft-lb

M_Z yawing moment, $I_Z\ddot{\psi}$, ft-lb

P period of oscillation, sec

p pressure, lb/sq ft

q dynamic pressure, lb/sq ft; pitching velocity, radians/sec

S total wing area (including area enclosed in fuselage), sq ft

t time, sec

$T_{1/2}$ time to damp to one-half amplitude, sec

V free-stream velocity, ft/sec

W weight of model, lb

X longitudinal body axis

Y lateral body axis

Z normal body axis

α angle of attack, deg

$\dot{\alpha}$ time rate of change of angle of attack, $\frac{1}{57.3}\frac{\partial \alpha}{\partial t}$, radians/sec

β angle of sideslip, deg

γ flight-path angle, deg

ϵ inclination of principal axes, deg

θ angle of pitch, radians

$\dot{\theta}$ time rate of change of angle of pitch, $\frac{\partial \theta}{\partial t}$, radians/sec

$\ddot{\theta}$ pitching acceleration, $\frac{\partial^2 \theta}{\partial t^2}$, radians/sec^2

ϕ angle of roll, radians

$\ddot{\phi}$ roll acceleration, $\frac{\partial^2 \phi}{\partial t^2}$, radians/sec^2

ψ angle of yaw, deg

$\ddot{\psi}$ yawing acceleration, $\frac{1}{57.3}\frac{\partial^2 \psi}{\partial t^2}$, radians/sec^2

Derivatives

$C_{L_\alpha} = \frac{\partial C_L}{\partial \alpha}$, per deg

$C_{m_\alpha} = \frac{\partial C_m}{\partial \alpha}$ (from two-accelerometer method), per deg

$$C_{m_\alpha} = -\frac{I_Y}{57.3qS\bar{c}}\left[\frac{4\pi^2}{P^2} + \left(\frac{0.693}{T_{1/2}}\right)^2\right]$$

(from two-degree-of-freedom method), per deg

$$C_{m_{\dot{\alpha}}} = \frac{\partial C_m}{\partial \frac{\dot{\alpha}\bar{c}}{2V}}, \text{ per radian}$$

$$C_{m_q} = \frac{\partial C_m}{\partial \frac{q\bar{c}}{2V}}, \text{ per radian}$$

$$C_{m_q} + C_{m_{\dot{\alpha}}} = -\frac{4I_Y V}{qS\bar{c}^2}\left(\frac{0.693}{T_{1/2}} - \frac{57.3C_{L_\alpha}qS}{2mV}\right)$$

(from two-degree-of-freedom method), per radian

Subscripts:

b	base
cg	center of gravity
F	fuselage
∞	free stream
T	horizontal tail
W	wing

MODEL AND INSTRUMENTATION

Model

A three-view drawing of the model is shown in figure 2. Photographs of the model are shown in figure 3. The low-position, steel, delta wing

had a leading-edge sweepback of 52.5°, a taper ratio of zero, and NACA 65A003 airfoil sections in the streamwise direction. The steel unswept horizontal tail had fixed incidence of -3.0° with respect to the fuselage center line and had -10° dihedral. The steel vertical tail had the quarter-chord line swept back 60°. Horizontal and vertical tail surfaces had hexagonal airfoil sections. Areas and aspect ratios given in figure 2 are based on theoretical dimensions.

The aluminum-alloy fuselage consisted of an ogive nose section, a cylindrical 5.0-inch-diameter center section and a boattailed tail section. The canopy was constructed of sheet steel. Fuselage and canopy ordinates are given in table I. Housed in the nose section of the model were electrically actuated pitch disturber vanes (which can be seen in fig. 3(a)).

The model weighed 108.6 pounds and had moments of inertia in pitch, yaw, and roll of 9.48, 9.54, and 0.30 slug-ft^2, respectively. Inclination of the principal axis was 2.8° below the body axis at the nose. The center of gravity was located at a station corresponding to 21 percent of the wing mean aerodynamic chord. The ratio of base area to wing area was 0.0226.

Instrumentation

The model was equipped with an NACA telemetering system which transmitted continuous measurements of normal accelerations at two reference stations, transverse accelerations at two reference stations, longitudinal acceleration, angle of attack, angle of sideslip, rate of roll, total pressure, reference static pressure, and base pressure.

In addition to the instrumentation carried internally, the model was tracked by a CW Doppler velocimeter and an NACA modified SCR-584 radar set to provide the velocity of the model and trajectory data, respectively. Atmospheric and wind conditions were determined by means of a radiosonde launched near the time of flight and tracked by a Rawin set.

FLIGHT TEST AND ANALYSIS

Flight Test

The model was launched at an angle of approximately 65° from the horizontal by means of a modified 90-millimeter gun mount launcher as shown in figure 3(c). The three-stage vehicle consisted of two

6-inch-diameter solid-propellant ABL Deacon rocket motors as the first stage, two more Deacon rocket motors as the second stage, and the non-sustained model mounted below and on the second stage as the third stage.

The first stage boosted the model—second-stage combination to a Mach number of about 1.20. The second stage was ignited at burnout of the first stage by means of self-contained batteries and a separation switch, and boosted the model to the maximum Mach number. The model was locked to the second stage during burning of the first stage to prevent premature separation. At ignition of the second stage, pressure from one of the second-stage rocket motors unlocked the model to permit separation at second-stage burnout. All reported measurements were obtained during the decelerating portion of the model flight.

The variations of dynamic pressure and Reynolds number (based on wing mean aerodynamic chord) with Mach number are shown in figure 4. The dynamic pressure and Reynolds number range covered were from about 600 to 8,300 lb/sq ft and about 3×10^6 to 19×10^6, respectively.

During the boosted phase of the flight, the pitch disturber vanes were retracted and were to begin operating shortly after model-booster separation. For some unknown reason the pitch disturber vanes failed to operate.

Analysis

Disturbances of the model from trim conditions in the longitudinal mode are usually analyzed by a method such as reference 1 which assumes, essentially, two degrees of freedom. In the present investigation, because of failure of the disturbing mechanism, the only model disturbance was caused by model separation from the second-stage booster rocket motor. Although the disturbance was primarily in the longitudinal mode (see fig. 5), some lateral oscillations were induced. If coupling between the longitudinal and lateral oscillations exists, the two-degree-of-freedom method of determining static and dynamic stability is invalid. An indication of coupled motions can be found by comparing the two-degree-of-freedom (period) static stability parameter C_{m_α} with the slope of C_m against α as determined from the two-accelerometer method (described in ref. 2).

Presented in figure 6 at average Mach numbers of 2.59, 2.63, 2.68, and 2.74 are the variations of C_m with α as determined from the two-accelerometer method compared with the slopes C_{m_α} as determined from

the two-degree-of-freedom method. The slopes from both methods are in good agreement. This indicates that the lateral oscillations have little effect on the longitudinal motions; however, the reverse is not necessarily true.

Near maximum Mach number where oscillations occurred, the longitudinal static stability was determined from the two-accelerometer method and the dynamic stability was determined from the two-degree-of-freedom method. The lateral oscillations, being relatively small in magnitude, were not analyzed.

CORRECTIONS AND ACCURACY

Measured quantities obtained from the instrumentation were corrected for instrument position off the center of gravity. Corrections for model pitching and yawing velocities were also made (by the method of ref. 3) to the readings of the air-flow indicator to obtain angles of attack and angles of sideslip.

Because instruments cannot be calibrated during or after flight, the absolute accuracy of the measured quantities is impossible to establish. Since CW Doppler radar is believed to be in error by less than 1 percent and peak velocity was determined by a CW Doppler radar set, peak Mach number should be accurate to about ±1 percent. Mach number subsequent to peak was determined from CW Doppler radar and from model instrumentation and is believed to be accurate to about ±3 percent at $M = 1.4$. An indication of the systematic instrument errors possible at trim conditions is given by the following table, based on an accuracy of ±1 percent of the full instrument range: (Coefficient errors due to dynamic-pressure inaccuracies are included.)

	Error at -	
	$M = 2.7$	$M = 1.4$
C_N	±0.005	±0.064
C_C	±0.001	±0.014

An indication of random errors encountered may be noted from the scatter of data points shown in the figures. Errors in angle of attack are independent of dynamic pressure and are not likely to vary with Mach number. Trim angles are estimated to be accurate within ±0.50°.

RESULTS AND DISCUSSION

The results obtained from the present investigation are shown in figures 4 to 10. Variations of aerodynamic center and lift-curve slope with Mach number are shown in figure 11. Also shown in this figure are the results of references 4 and 5, and theoretical calculations as determined from reference 6.

Time History

A time history of some of the quantities obtained in the present investigation is shown in figure 5. The large disturbance near peak Mach number was caused by separation of the model from the second-stage booster. It may be noted that although the oscillations are primarily in the longitudinal mode, some lateral oscillations are present. The lateral oscillations are generally of small magnitude and do not appear to affect the motions in the longitudinal mode. (See figs. 5 and 6.)

Lift, drag, and longitudinal static and dynamic stability were determined from the oscillations near peak Mach number. Base pressure, total drag, lift, and angles of attack at trim conditions were determined over the Mach number range covered ($M = 1.40$ to 2.78).

Trim Characteristics

The variations at model trim conditions of the base pressure coefficient, total drag coefficient, lift coefficient, and angle of attack as a function of Mach number are shown in figure 7. Calculations of base drag coefficient (obtained from base pressure coefficient) indicated a near constant value of about 0.002 or about 5 percent of the total trim drag coefficient at $M = 1.5$. Over the Mach number range covered ($M = 1.40$ to 2.78), the trim lift coefficient and angle of attack varied from about 0.12 to 0.04 and 3.8° to 2.0°, respectively.

Lift

Since the Mach number varied about 0.2 during the time required by the model to damp the disturbance near peak Mach number, the oscillations were divided into four Mach number sections. The variation of the lift coefficient with angle of attack at average Mach numbers of 2.59, 2.63, 2.68, and 2.74 is shown in figure 8. Generally, the lift-curve slopes varied linearly with angle of attack. Lift-curve slopes represented by the faired lines in figure 8 are presented as functions of Mach number in figure 11.

Drag

The variation of total drag coefficient with lift coefficient at the four average Mach numbers is shown in figure 9. It should be pointed out that drag coefficients were computed with sideslip and side-force effects neglected since calculations showed that these effects were small. At Mach numbers near 2.7, the value of the minimum drag coefficient was about 0.031 with lift coefficients for minimum drag near zero. The maximum lift-drag ratio and the lift coefficient for maximum lift-drag ratio at $M = 2.74$ were about 4.0 and 0.30, respectively. The base drag was approximately 5 percent of the model total trim drag.

Longitudinal Static Stability

The variation of the total pitching-moment coefficient (as determined from the two-accelerometer method) with lift coefficient at the four average Mach numbers is shown in figure 10. The pitching-moment coefficients presented herein are total; that is, they include the damping-in-pitch term $C_{m_q} + C_{m_{\dot{\alpha}}}$. In the present investigation, the effect of the damping-in-pitch term on the slope of the pitching-moment curve is believed to be small.

As with the lift-curve slopes, the pitching-moment curves are generally linear over the lift and Mach number range covered. Aerodynamic-center locations obtained from the slopes of the pitching-moment curves (fig. 10) are presented as a function of Mach number in figure 11.

Damping in Pitch

The damping-in-pitch parameter $C_{m_q} + C_{m_{\dot{\alpha}}}$, as determined from the two-degree-of-freedom method, varied from about -7.0 at $M = 2.59$ and 2.63 to about -3.5 at $M = 2.68$ and 2.74. Because of the small amplitudes of the oscillations at $M = 2.59$ and 2.63, the accuracy of the values of $C_{m_q} + C_{m_{\dot{\alpha}}}$ is in doubt and it is therefore believed that the value of about -3.5 obtained at the higher Mach numbers is indicative of the damping characteristics of the model configuration.

Theoretical Comparisons

As stated before, because of failure of the pitch disturbance mechanism, lift-curve slopes, minimum drag, and static and dynamic stability were obtained only near maximum Mach number. The results from two

rocket-propelled models having a $52\frac{1}{2}^{\circ}$ delta wing and a low, swept horizontal tail (refs. 4 and 5) have been included in this paper to give indications of lift-curve slope and aerodynamic-center variations at Mach numbers lower than those covered in the present test.

The variations of experimental and calculated aerodynamic-center locations and lift-curve slopes are presented in figure 11 as a function of Mach number. The experimental results were obtained from the present investigation and reference 4. Calculated results were determined from the theory of reference 6. The reference 4 data were corrected for flexibility by using the results of reference 5. The present test data were not corrected for flexibility since most of the corrections to the reference data were due to the aluminum-alloy tail. It should be pointed out that the data shown in figure 11 were taken at trim conditions with both models at a tail setting of about -3°.

Also included in figure 11 is a plan-form view of the model of the present investigation and the scaled model of references 4 and 5 superposed on each other. Except for horizontal-tail design, the two configurations are similar in the plan-form view. However, several features are dissimilar; for instance, the present model had a canopy, the wing in a low position, and the mean aerodynamic chord of the tail located above the wing chord plane. The reference models had no canopy, the wing in a midposition, and the mean aerodynamic chord of the tail below the wing chord plane. Also, there was a difference in the ratio of wing span to fuselage diameter between the two configurations. The results of reference 7 show that over a Mach number range of 0.61 to 1.90, wing position has little effect on the lift and aerodynamic-center location of the wing-fuselage combination; therefore, differences in lift and aerodynamic-center location for the complete models would be due to differences in the ratio of wing span to fuselage diameter and in the horizontal-tail plan form and location.

Theoretical calculations of aerodynamic center are in good agreement with experimental results when considering the theory accuracy of 0.02 of the fuselage length (about 10 percent $\bar{c}$ for both configurations). At Mach numbers where comparisons can be made, the theory predicts that both configurations have about the same static stability. From the standpoint of stability, differences in the ratio of wing span to fuselage diameter, horizontal-tail plan form, length, and height between the two configurations appear to be compensating.

Theoretical calculations of lift-curve slope are in very good agreement with experimental results. The difference in the theoretical values of C_{L_α} between the two complete models is primarily due to the difference in the values of C_{L_α} of the wing plus fuselage. The trend of the

theoretical lift-curve slopes from $M = 1.40$ to 1.78 is the same for both configurations with the present model having higher values of C_{L_α} than the model of reference 4.

Theoretical values of lift-curve slope and experimental reference values of aerodynamic-center location are believed indicative, at least at supersonic speeds, of those that would have been obtained from the present test configuration at lower Mach numbers.

CONCLUDING REMARKS

A free-flight investigation of an airplane configuration having a low 52.5° delta wing and an unswept horizontal tail has been conducted over a Mach number range of 1.40 to 2.78. Because the pitch disturbance mechanism failed to operate, a disturbance from trim conditions was obtained only at separation from the second-stage rocket motors near maximum Mach numbers. The disturbance was primarily in the longitudinal mode and only the longitudinal oscillations were analyzed. Base pressure, lift, and drag coefficients and angles of attack were obtained over the Mach number range covered.

At a fixed tail setting of -3.0°, the trim lift coefficient and angle of attack varied from about 0.12 to 0.04 and 3.8° to 2.0°, respectively. The base drag was approximately 5 percent of the total trim drag.

The longitudinal oscillations covered a Mach number range of 2.59 to 2.74. Theoretical calculations of lift-curve slope and aerodynamic-center location were in good agreement with experimental results.

Langley Aeronautical Laboratory,
National Advisory Committee for Aeronautics,
Langley Field, Va., January 7, 1958.

REFERENCES

1. Gillis, Clarence L., Peck, Robert F., and Vitale, A. James: Preliminary Results From a Free-Flight Investigation at Transonic and Supersonic Speeds of the Longitudinal Stability and Control Characteristics of an Airplane Configuration With a Thin Straight Wing of Aspect Ratio 3. NACA RM L9K25a, 1950.

2. Vitale, A. James: Effects of Wing Elasticity on the Aerodynamic Characteristics of an Airplane Configuration Having 45° Sweptback Wings As Obtained From Free-Flight Rocket-Model Tests at Transonic Speeds. NACA RM L52L30, 1953.

3. Mitchell, Jesse L., and Peck, Robert F.: An NACA Vane-Type Angle-of-Attack Indicator for Use at Subsonic and Supersonic Speeds. NACA TN 3441, 1955. (Supersedes NACA RM L9F28a.)

4. Kehlet, Alan B.: Aerodynamic Characteristics at Transonic and Supersonic Speeds of a Rocket-Propelled Airplane Configuration Having a 52.5° Delta Wing and a Low, Swept Horizontal Tail. NACA RM L54A20, 1954.

5. Kehlet, Alan B.: Free-Flight Investigation Over a Mach Number Range From 0.74 to 1.43 at Lift Coefficients From -0.15 to 0.75 of an Airplane-Configuration Model Having a 52.5° Delta Wing and a Low Swept Horizontal Tail. NACA RM L56G09, 1956.

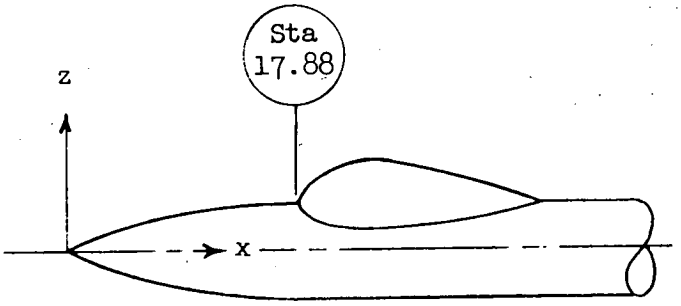
6. Nielsen, Jack N., Kaattari, George E., and Anastasio, Robert F.: A Method for Calculating the Lift and Center of Pressure of Wing-Body-Tail Combinations at Subsonic, Transonic, and Supersonic Speeds. NACA RM A53G08, 1953.

7. Heitmeyer, John C.: Effect of Vertical Position of the Wing on the Aerodynamic Characteristics of Three Wing-Body Combinations. NACA RM A52L15a, 1953.

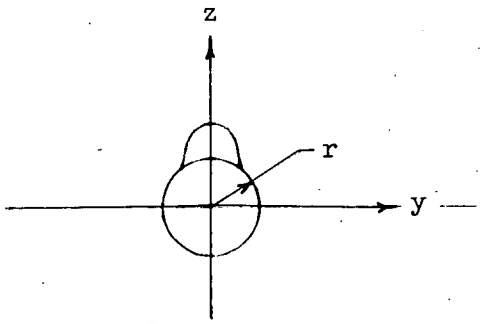
TABLE I.- FUSELAGE AND CANOPY ORDINATES

Fuselage ordinates	
x	r
0.000	0.000
.500	.141
1.500	.410
2.500	.663
3.500	.900
4.500	1.120
5.500	1.324
6.500	1.512
6.605	1.531
7.500	1.684
8.500	1.839
9.500	1.978
10.500	2.100
11.500	2.206
12.500	2.296
13.500	2.369
14.500	2.427
15.500	2.467
16.500	2.492
16.625	2.493
17.500	2.500
64.105	2.500
64.980	2.493
65.105	2.492
66.105	2.467
67.105	2.427
68.105	2.369
69.105	2.296
70.105	2.206
71.105	2.100
72.105	1.978
73.105	1.839
74.105	1.684
75.000	1.531

Canopy ordinates		
x	±y	z
17.88	0.00	2.50
19.00	1.19	3.15
20.25	1.64	3.66
22.00	1.85	4.05
24.75	1.73	4.00
27.00	1.47	3.72
29.00	1.20	3.43
31.25	.73	3.02
33.75	.00	2.50



Side view



Rear view

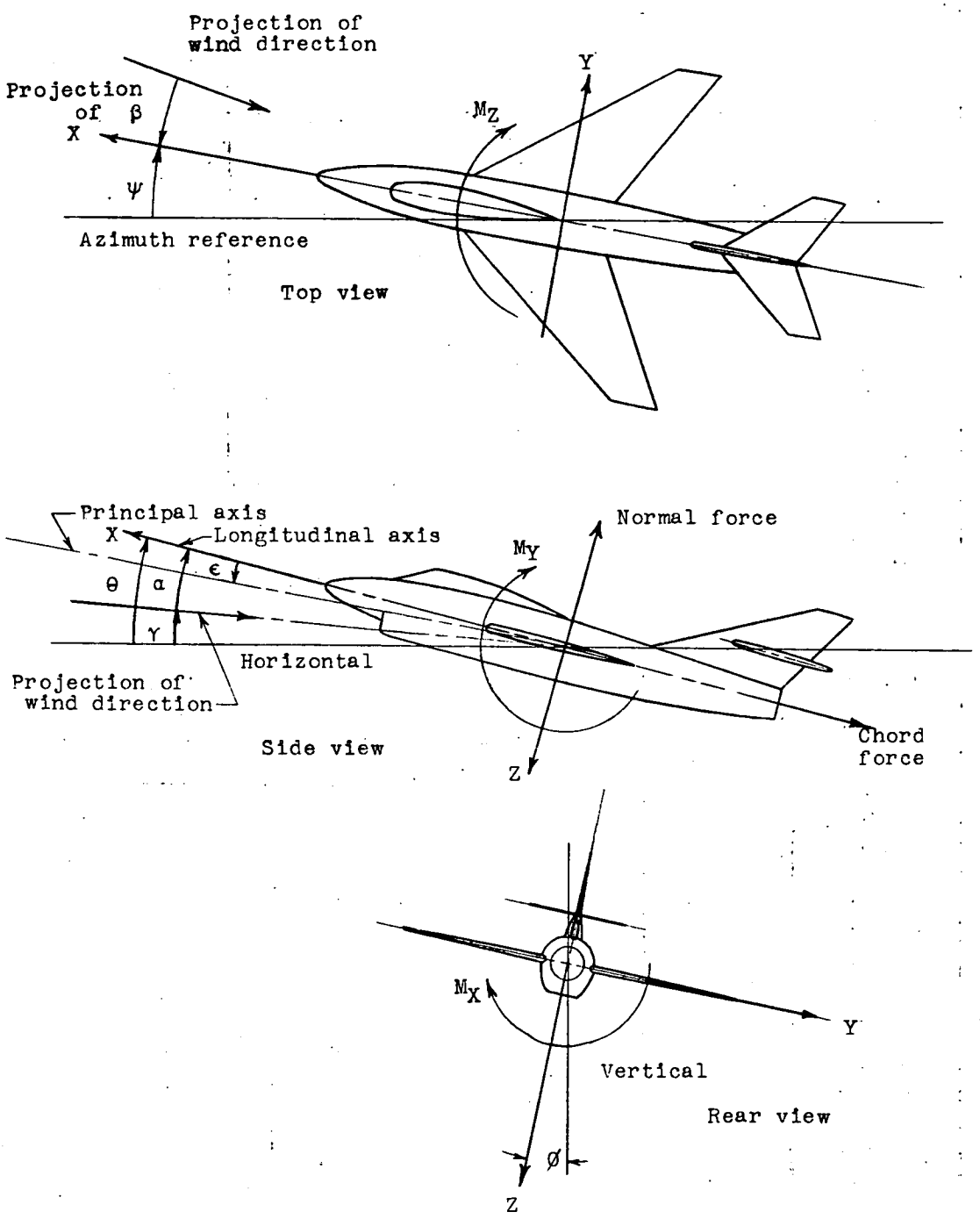


Figure 1.- System of body axes and angular relationships. Each view presents a plane of the axes system as viewed along and in a positive direction of the third axis.

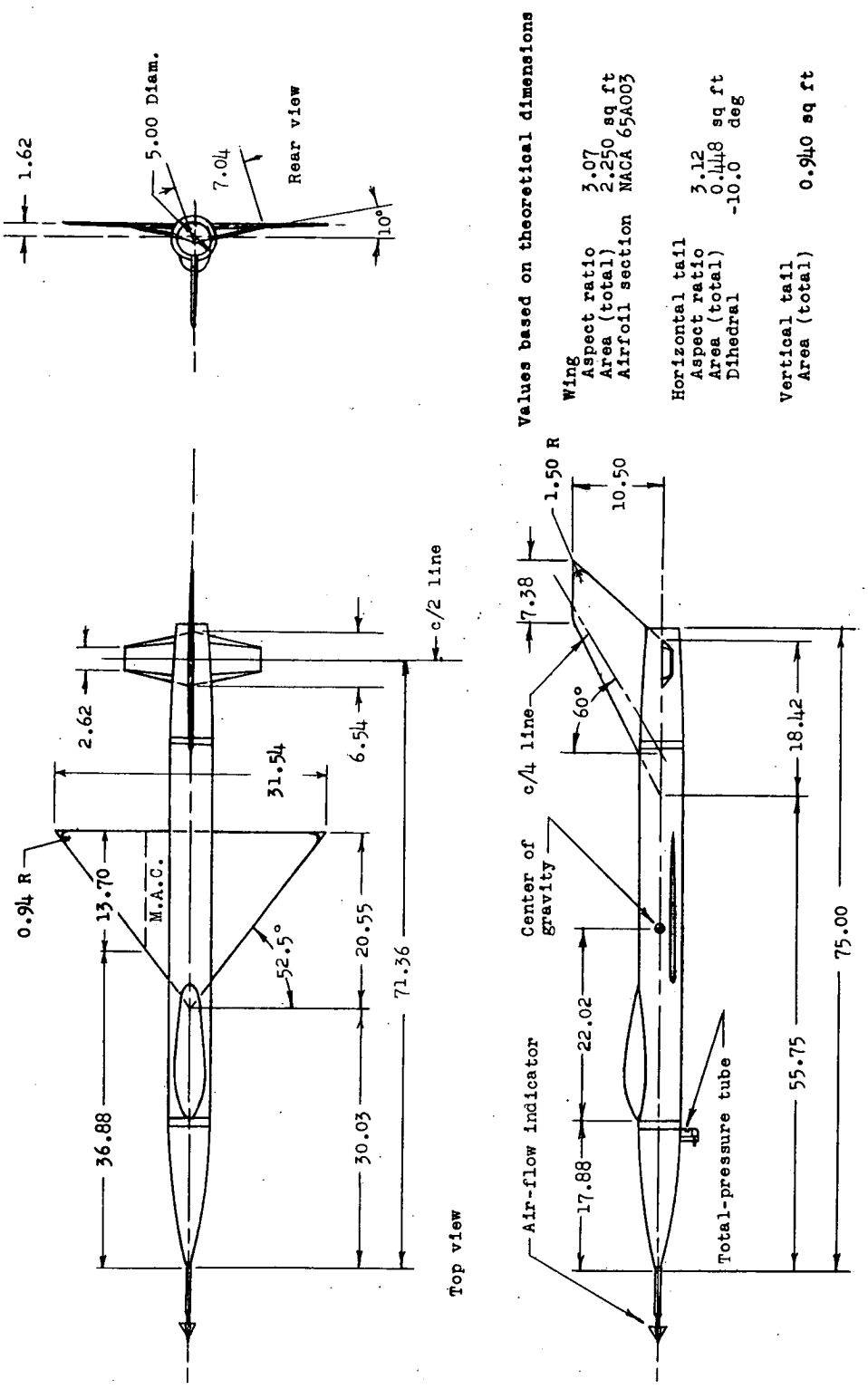
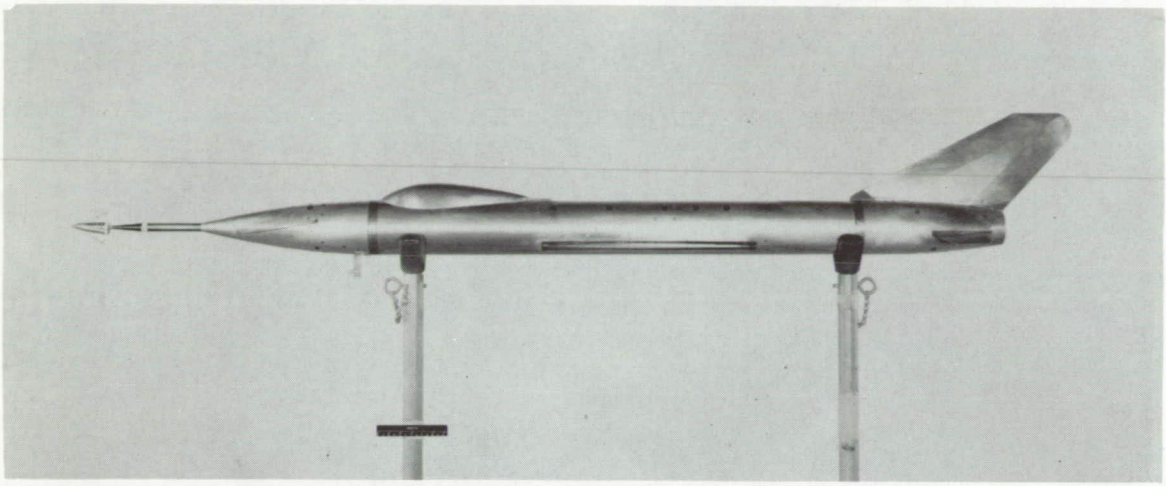
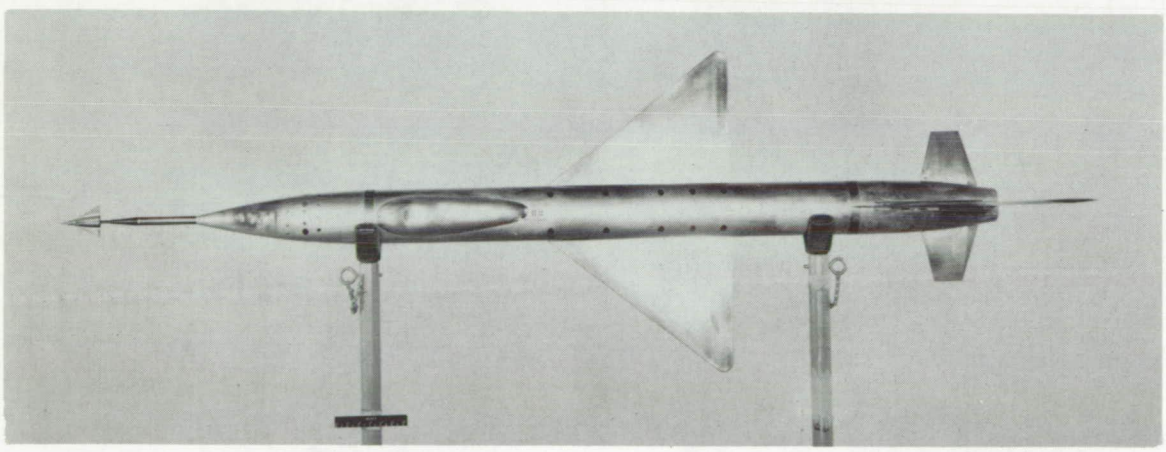


Figure 2.- General arrangement of model. All dimensions are in inches.

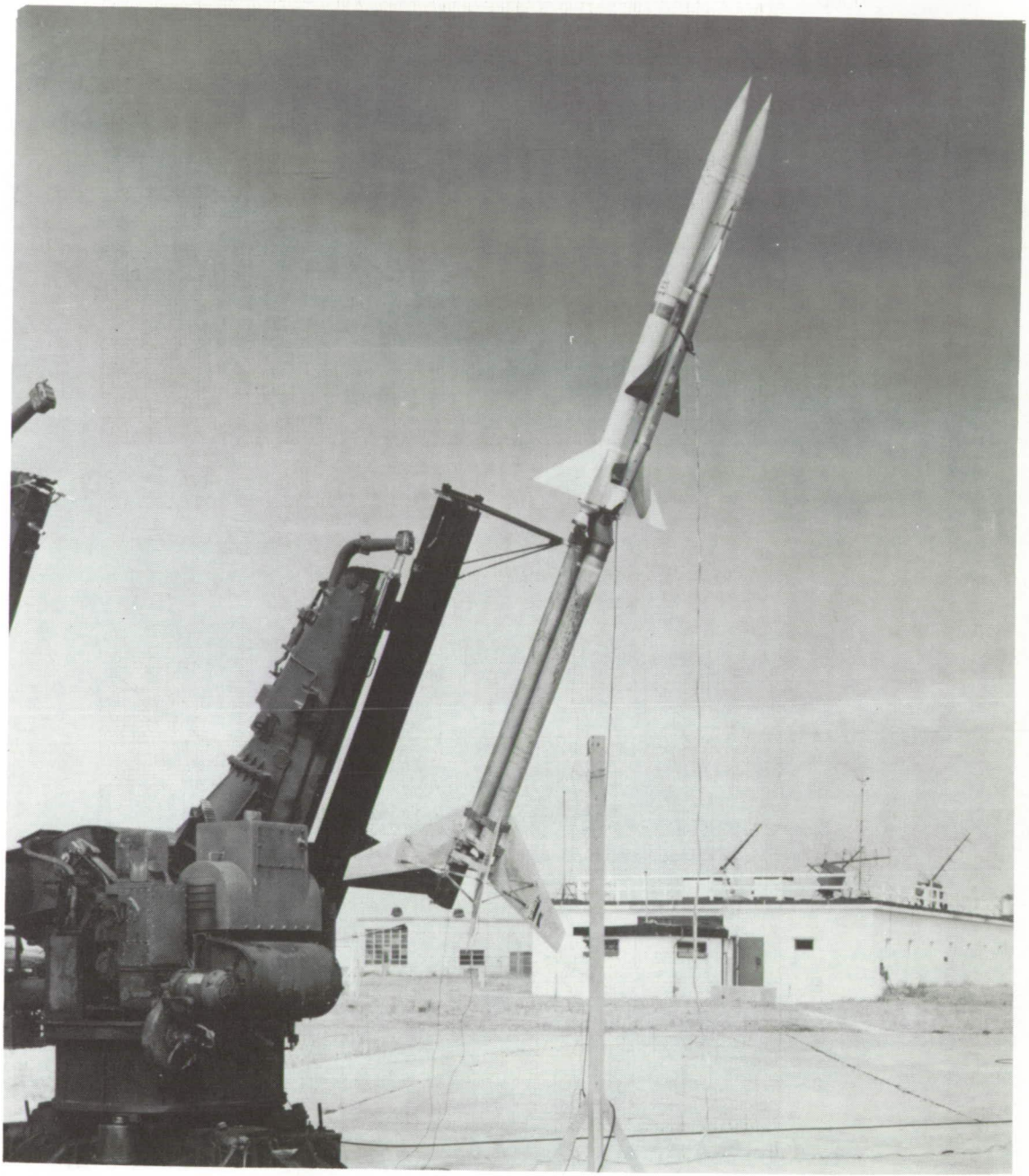


(a) Side view. L-92207.1



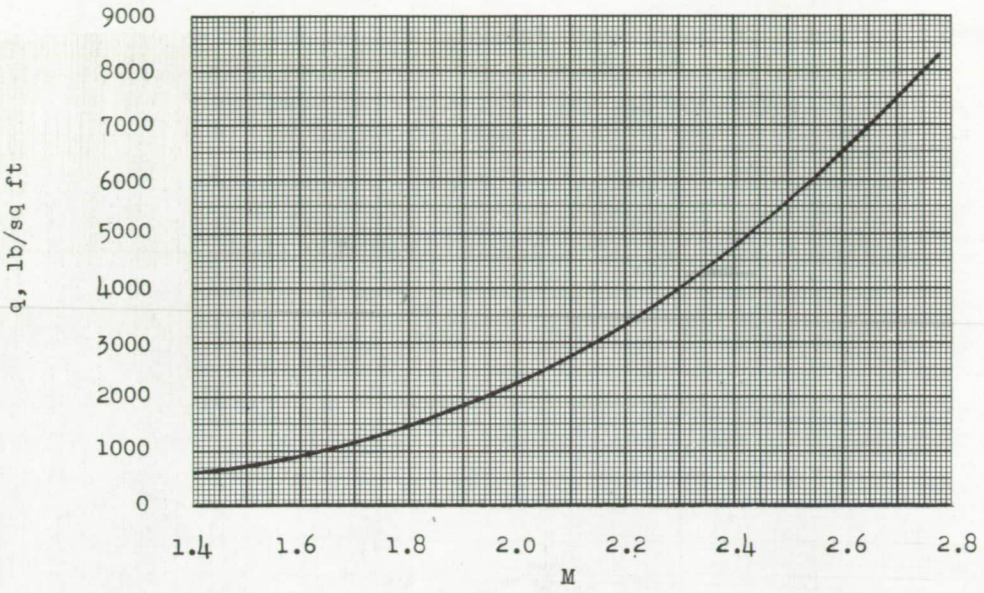
(b) Top view. L-92206.1

Figure 3.- Photographs of the model and model-booster combination.

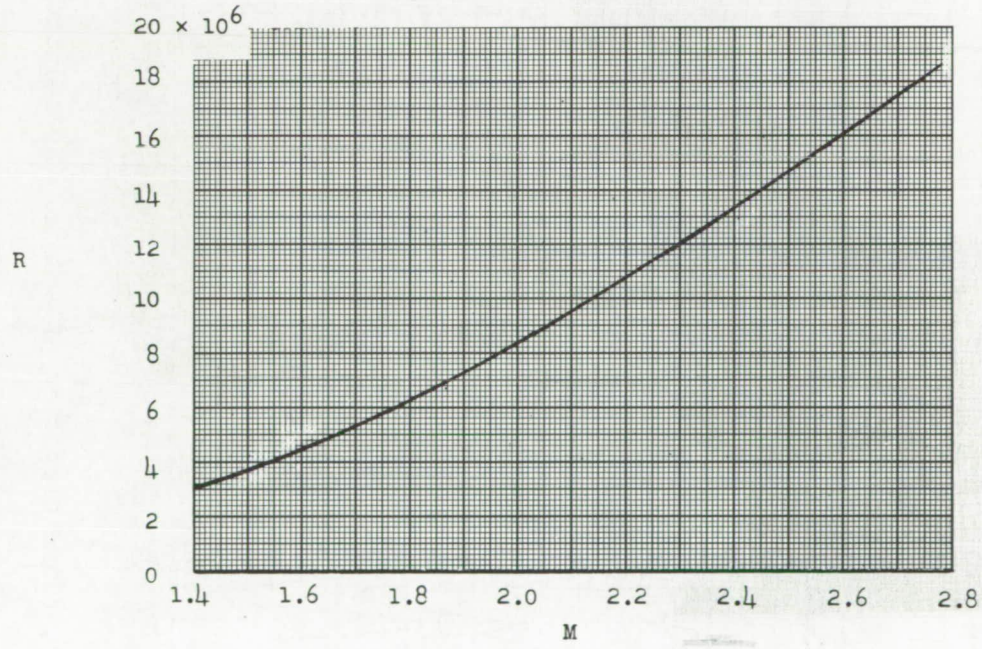


(c) Model and booster combination on launcher. L-92560.1

Figure 3.- Concluded.



(a) Dynamic pressure.



(b) Reynolds number.

Figure 4.- Variation of dynamic pressure and Reynolds number with Mach number.

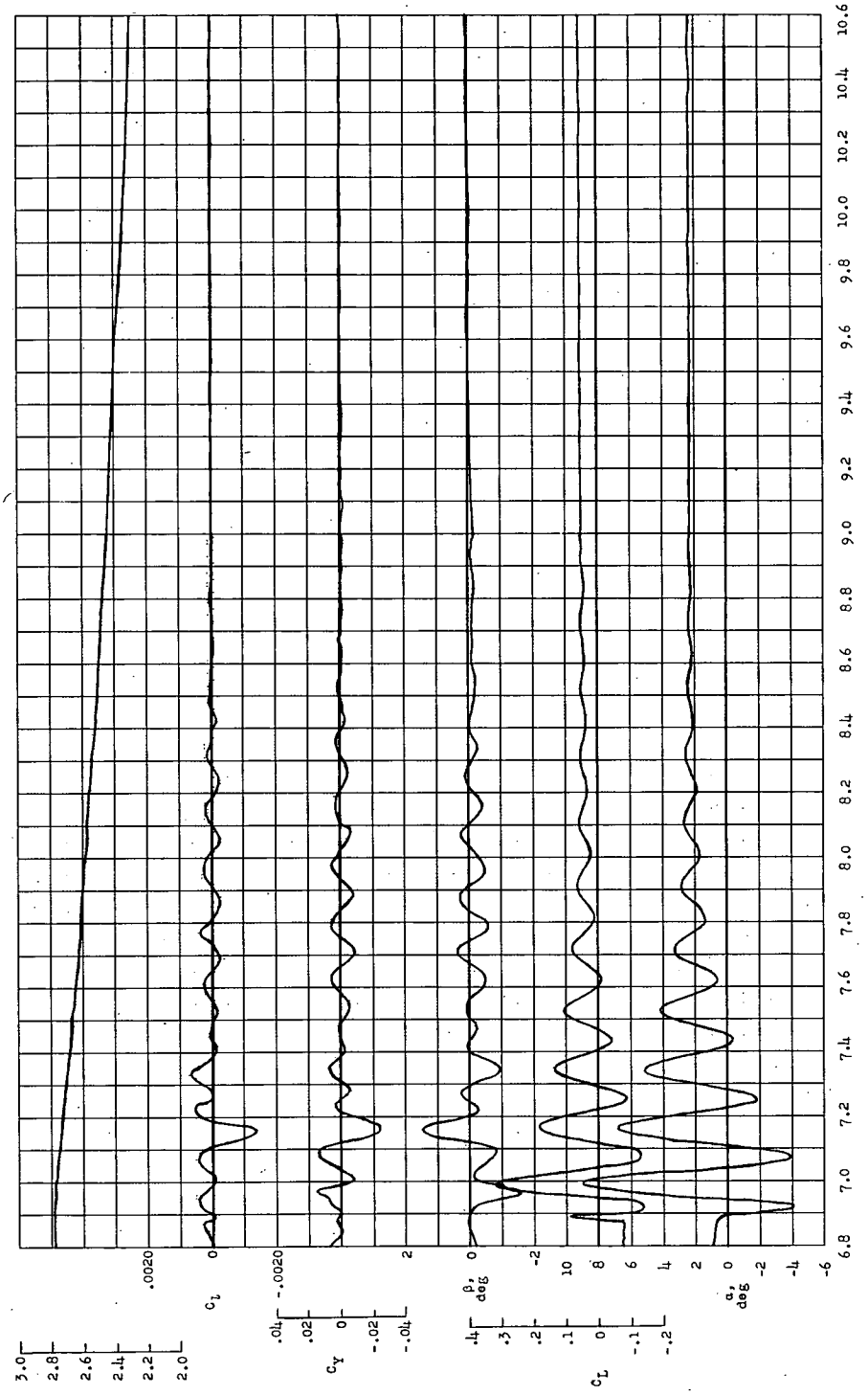


Figure 5.- Time histories of some of the quantities obtained during investigation.

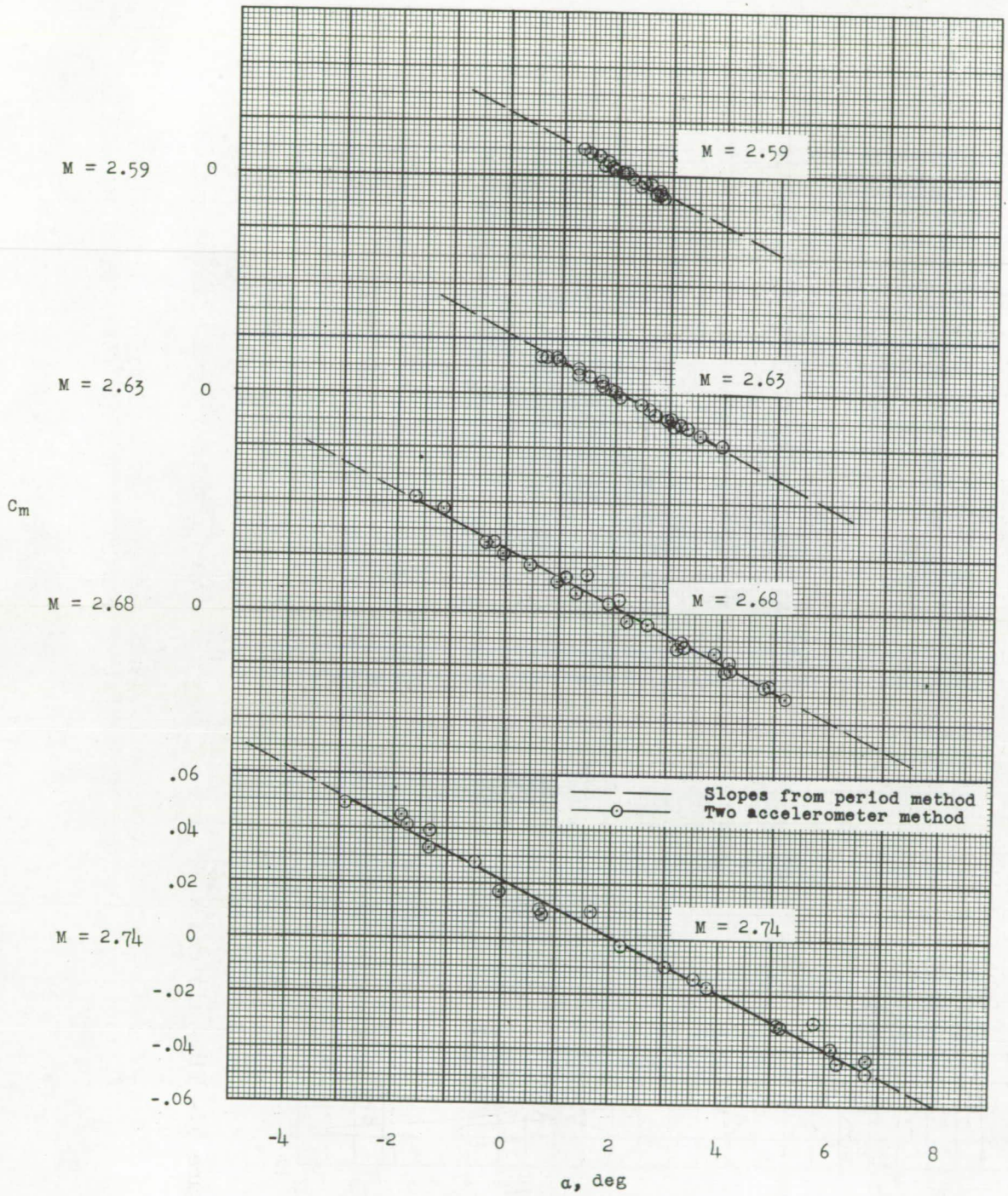


Figure 6.- Variation of the total pitching-moment coefficient with angle of attack.

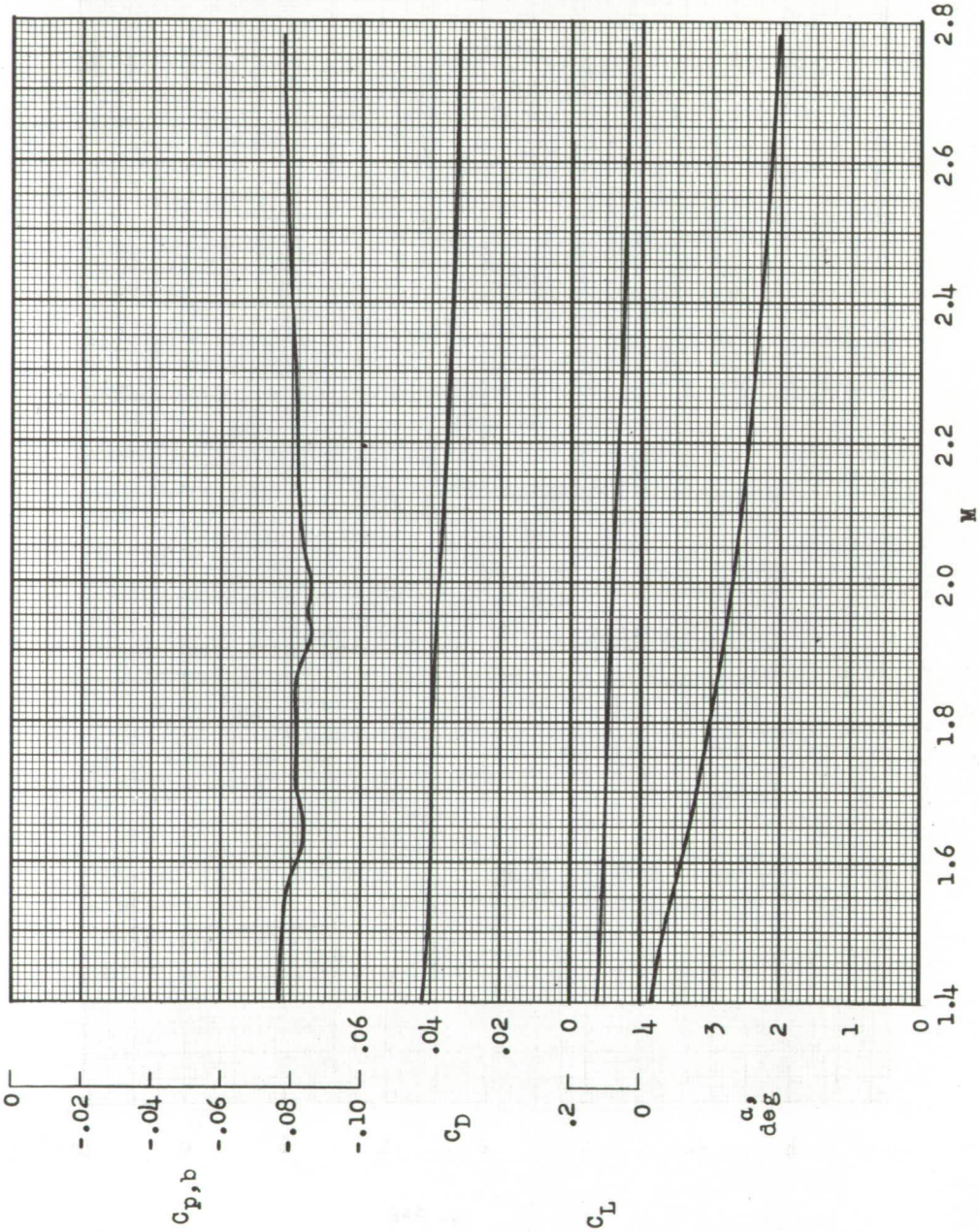


Figure 7.- Base pressure coefficient, total drag coefficient, lift coefficient, and angle of attack at trim conditions as a function of Mach number.

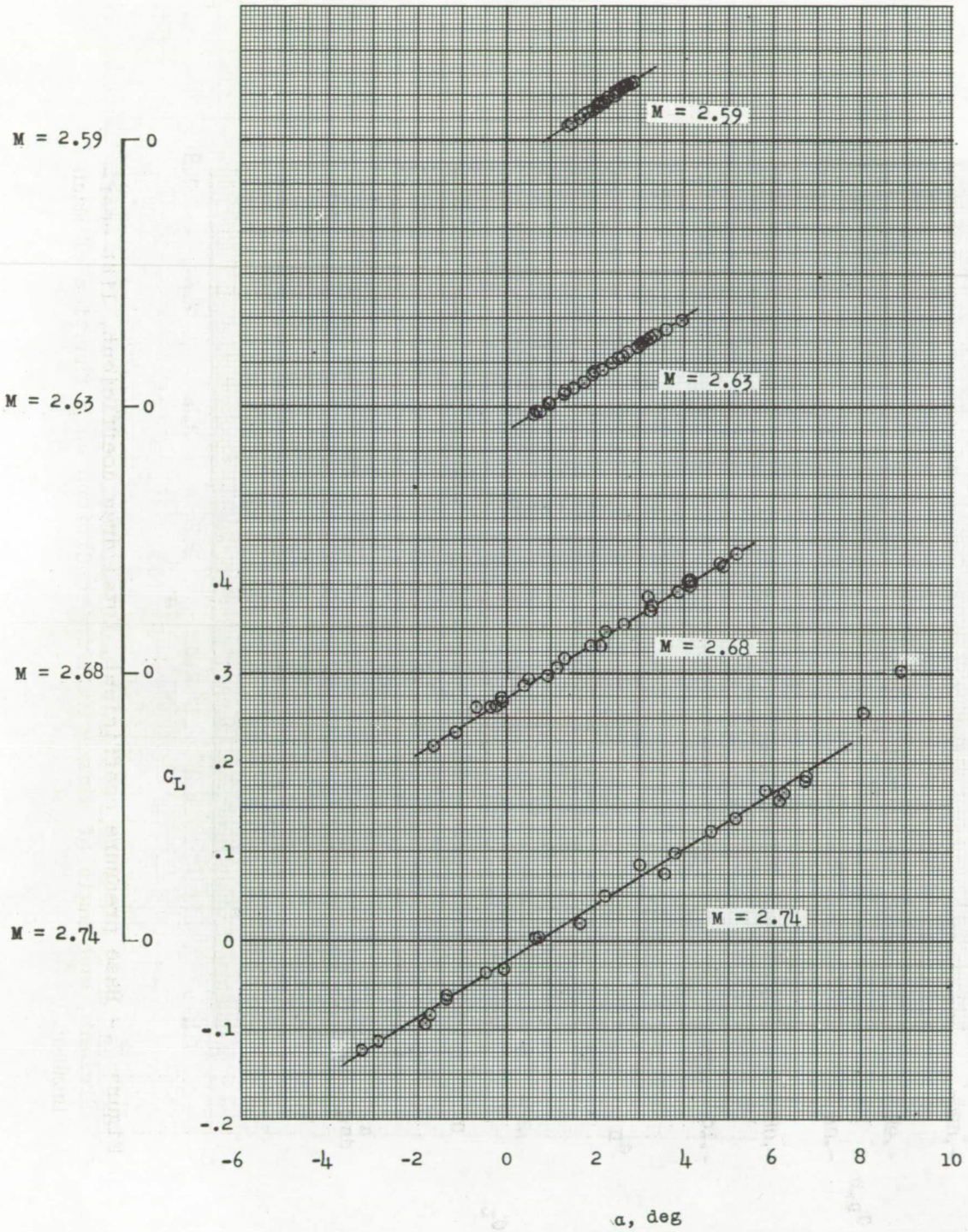


Figure 8.- Variation of lift coefficient with angle of attack.

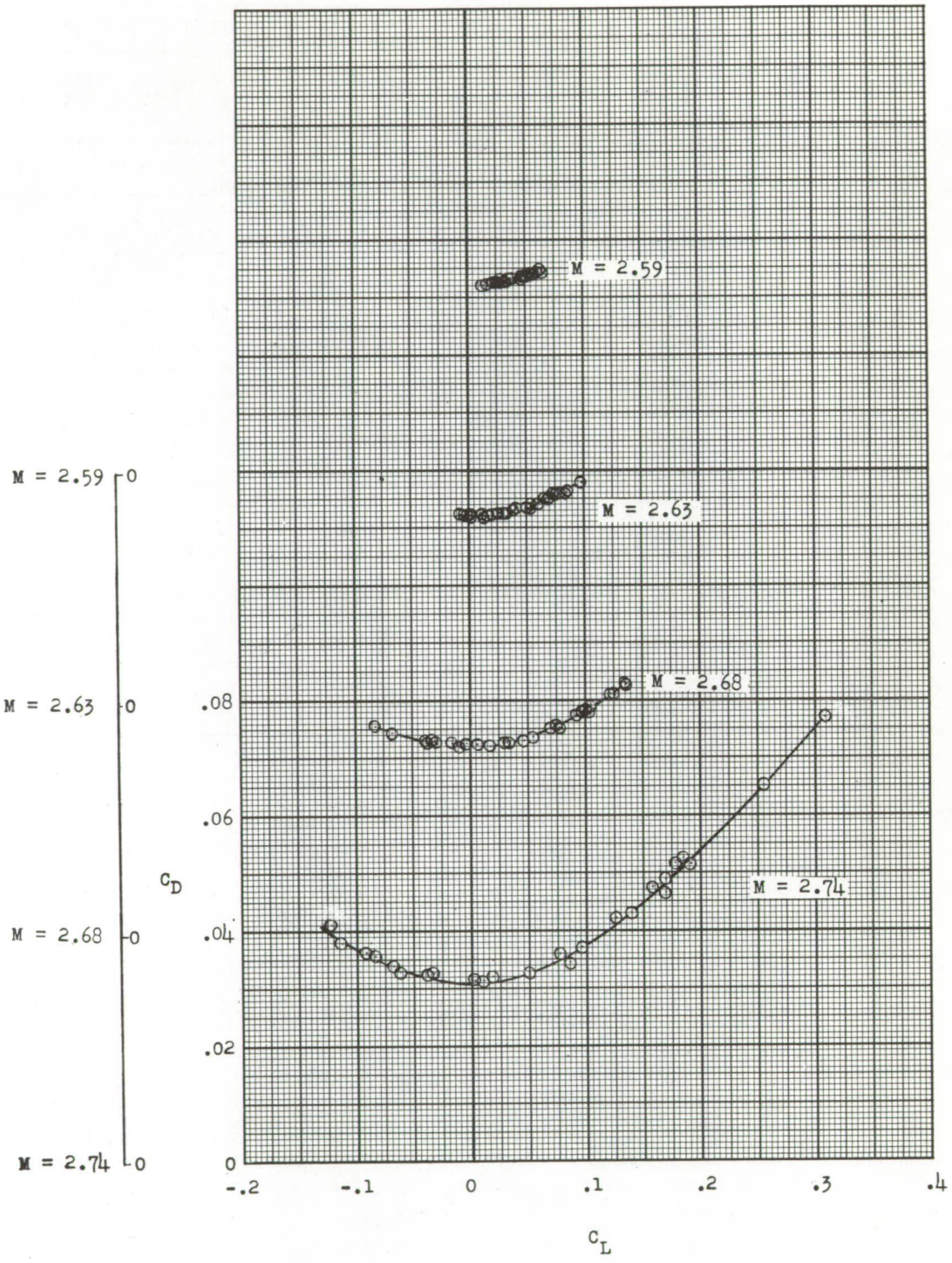


Figure 9.- Variation of total drag coefficient with lift coefficient.

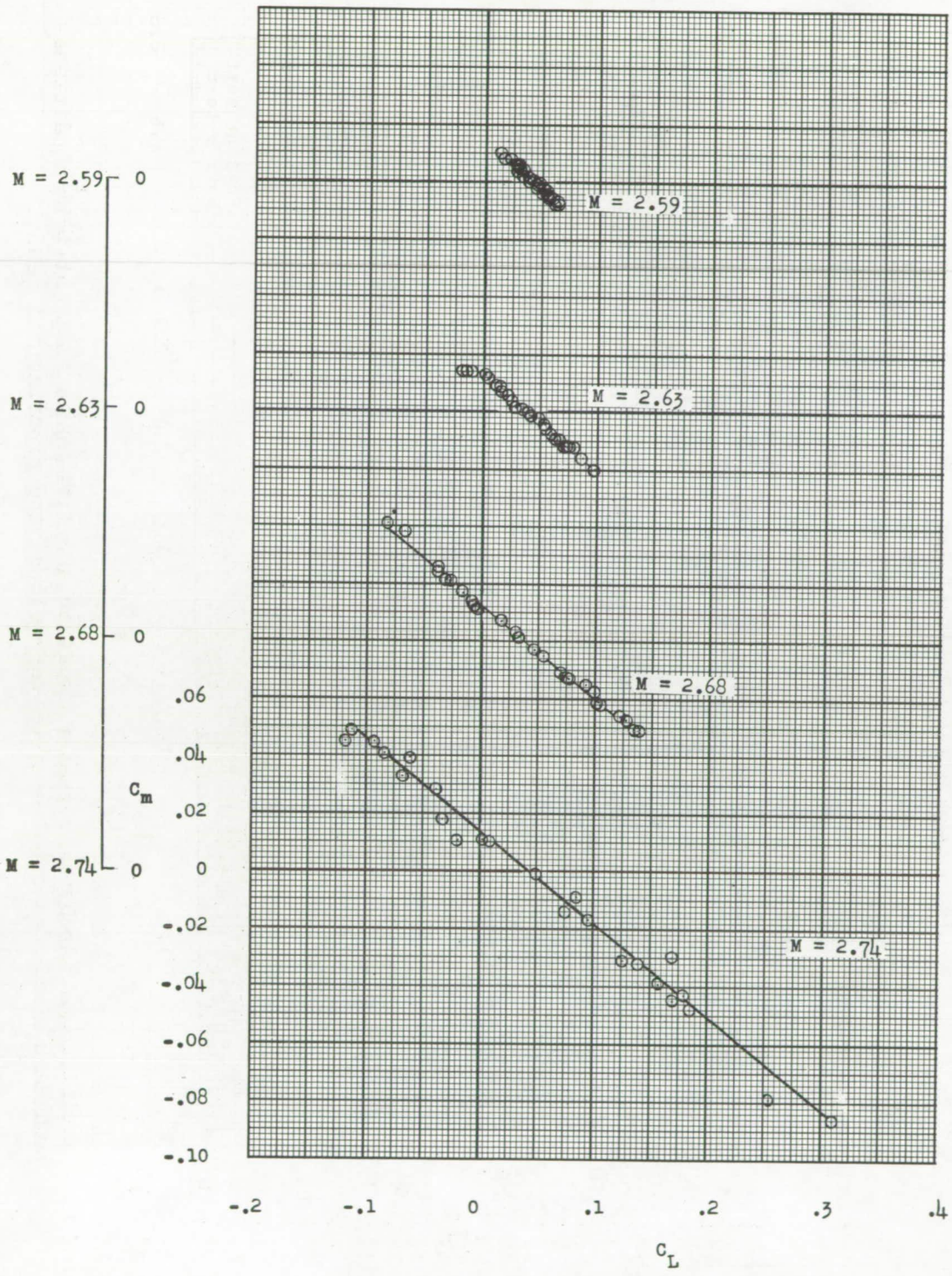


Figure 10.- Variation of the total pitching-moment coefficient with lift coefficient.

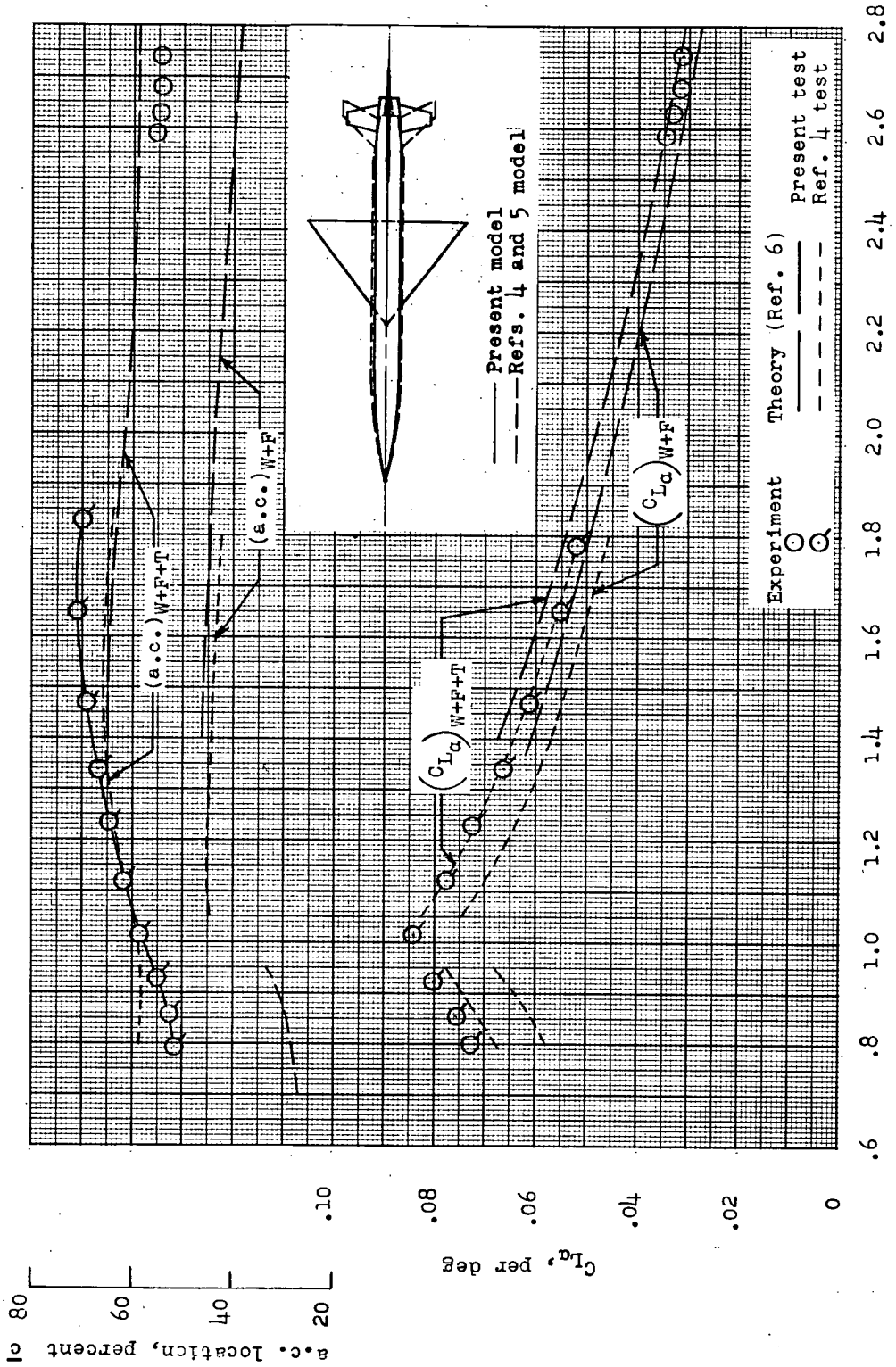


Figure 11.- Variation of aerodynamic-center location and lift-curve slope at trim conditions with Mach number as obtained from theoretical and experimental means.